Video Article

A Tripeptide-Stabilized Nanoemulsion of Oleic Acid

Sylwia A. Dragulska[1], Marek T. Wlodarczyk[1,2], Mina Poursharifi[1,3], John A. Martignetti[4,5,6], Aneta J. Mieszawska[1,2,3]

[1]Department of Chemistry, Brooklyn College, The City University of New York

[2]Ph.D. Program in Chemistry, The Graduate Center of The City University of New York

[3]Ph.D. Program in Biochemistry, The Graduate Center of The City University of New York

[4]Department of Genetics and Genomic Sciences, Icahn School of Medicine at Mount Sinai

[5]Women's Health Research Institute, Icahn School of Medicine at Mount Sinai

[6]Laboratory for Translational Research, Western Connecticut Health Network

Correspondence to: Aneta J. Mieszawska at Aneta.Mieszawska@brooklyn.cuny.edu

URL: https://www.jove.com/video/59034
DOI: doi:10.3791/59034

Keywords: Nanoemulsion, oleic acid, tripeptide, anticancer therapy, biological imaging, drug delivery

Date Published: 12/21/2018

Citation: Dragulska, S.A., Wlodarczyk, M.T., Poursharifi, M., Martignetti, J.A., Mieszawska, A.J. A Tripeptide-Stabilized Nanoemulsion of Oleic Acid. *J. Vis. Exp.* (), e59034, doi:10.3791/59034 (2018).

Abstract

We describe a method to produce a nanoemulsion composed of an oleic acids-Pt(II) core and a lysine-tyrosine-phenylalanine (KYF) coating (KYF-Pt-NE). The KYF-Pt-NE encapsulates Pt(II) at 10 wt. %, has a diameter of 107 ± 27 nm and a negative surface charge. The KYF-Pt-NE is stable in water and in serum, and is biologically active. The conjugation of a fluorophore to KYF allows the synthesis of a fluorescent nanoemulsion that is suitable for biological imaging. The synthesis of the nanoemulsion is performed in an aqueous environment, and the KYF-Pt-NE forms via self-assembly of a short KYF peptide and an oleic acids-platinum(II) conjugate. The self-assembly process depends on the temperature of the solution, the molar ratio of the substrates, and the flow rate of the substrate addition. Crucial steps include maintaining the optimal stirring rate during the synthesis, permitting sufficient time for self-assembly, and pre-concentrating the nanoemulsion gradually in a centrifugal concentrator.

Introduction

In recent years, there has been a growing interest in the engineering of nanoparticles for such biomedical applications as drug delivery and bioimaging[1,2,3,4]. The multifunctionality of nanoparticle-based systems often necessitates incorporating multiple components within one formulation. The building blocks that are based on lipids or polymers often differ in terms of their physicochemical properties as well as their biocompatibility and biodegradability, which ultimately might affect the function of the nanostructure[1,5,6]. Biologically derived materials, such as proteins and peptides, have long been recognized as promising components of multifunctional nanostructures due to their sequence flexibility[7,8]. Peptides self-assemble into highly ordered supramolecular architectures forming helical ribbons[9,10], fibrous scaffolds[11,12], and many more, thus paving the way to building biomolecule-based hybrid nanostructures using a bottom-up approach[13].

Peptides have been explored for applications in medicine and biotechnology, especially for anticancer therapy[14] and cardiovascular diseases[15] as well as for antibiotic development[16,17], metabolic disorders[18], and infections[19]. There are over a hundred of small-peptide therapeutics undergoing clinical trials[20]. Peptides are easy to modify and fast to synthesize at low cost. In addition, they are biodegradable, which greatly facilitates their biological and pharmaceutical applications[21,22]. The use of peptides as structural components includes the engineering of responsive, peptide-based nanoparticles and hydrogel depots for controlled release[23,24,25,26,27], peptide-based biosensors[28,29,30,31], or bio-electronic devices[32,33,34]. Importantly, even short peptides with two or three amino-acid residues that include phenylalanine were found to guide the self-assembly processes[35,36,37] and create stabilized emulsions[38].

Platinum-based drugs, owing to their high efficacy, are used in many cancer treatment regimens, both alone and in combination with other agents[39,40]. Platinum compounds induce DNA damage by forming monoadducts and intrastrand or interstrand cross-links. The Pt-DNA lesions are recognized by the cellular machinery and, if not repaired, lead to cellular apoptosis. The most important mechanism, by which Pt(II) contributes to cancer cell death, is the inhibition of DNA transcription[41,42]. However, the benefits of platinum therapy are diminished by systemic toxicity of Pt(II) that triggers severe side effects. This leads to lower clinical dosing of Pt(II)[43], which often results in sub-therapeutic concentrations of platinum reaching the DNA. As a consequence, the DNA repair that follows contributes to cancer cell survival and acquiring Pt(II) resistance. The platinum chemo-resistance is a major problem in anticancer therapy and the main cause of treatment failure[44,45].

We have developed a stable nanosystem that encapsulates the Pt(II) agent in order to provide a shielding effect in systemic circulation and to diminish the Pt(II)-induced side effects. The system is based on an oleic acids-Pt(II) core stabilized with a KYF tripeptide to form a nanoemulsion (KYF-Pt-NE)[46]. The building blocks of KYF-Pt-NE, the amino acids of the tripeptide as well as the oleic acid, have the Generally Recognized As Safe (GRAS) status with Food and Drug Administration (FDA). The KYF-Pt-NE is prepared by using a nanoprecipitation method[47]. In short, the oleic acids-Pt(II) conjugate is dissolved in an organic solvent and then added dropwise to an aqueous KYF solution (**Figure 1**) at 37 °C. The solution is stirred for several hours to allow self-assembly of the KYF-Pt-NE. The nanoemulsion is concentrated in 10 kDa centrifugal

concentrators and washed three times with water. The chemical modification of the KYF with a fluorophore allows the synthesis of fluorescent FITC-KYF-Pt-NE suitable for biomedical imaging.

Protocol

1. Synthesis of the Oleic Acids–Platinum(II) Conjugate

1. Activation of cisplatin
    1. Suspend 50 mg (0.167 mmol) of cisplatin in 4 mL of water (e.g., nanopure) at 60 °C.
    2. Add dropwise 55.2 mg (0.325 mmol) of $AgNO_3$ in 0.5 mL of water to the solution of cisplatin and stir the reaction for at least 2 h at 60 °C. The white precipitate of AgCl will form indicating the progress of the reaction.
    3. To determine if the activation reaction is completed, perform the test with 10% HCl for the presence of free Ag^+ ion in solution. The test should be negative (no additional AgCl precipitate should form).
    4. Centrifuge the reaction mixture at 3,220 x *g* for 10 min and remove the white precipitate of AgCl.
    5. Collect the supernatant and filter it via a 0.2 mm syringe filter. Test the supernatant for the presence of platinum by applying 2-3 drops of the solution via Pasteur pipette to $SnCl_2$ crystals. The test is positive if the color of coordinate complex of tin with platinum is dark yellow/orange.
    6. Use the supernatant with activated Pt(II) for the second step.

2. Reaction of oleic acid with activated Pt(II)
    1. Dissolve 13.3 mg (0.333 mmol) of NaOH in 3 mL of water at 60 °C to obtain a 0.11 M solution.
    2. Add 94.2 mg of oleic acid (0.333 mmol) to 0.11 M NaOH, and mix with the solution of activated Pt(II) from step 1.1.
    3. Stir the reaction for 2 h at 60 °C and next at room temperature overnight. The crude product is an oily brown/yellow precipitate.
    4. Centrifuge the reaction mixture at 3,220 x *g* for 10 min and remove the supernatant. Dry the crude product at 25 °C using a rotary evaporator. Purify the product by multiple washes with acetonitrile. The final color of pure oleic acids–Pt(II) conjugate is pale yellow.

2. Synthesis of KYF-Pt-NE, and the FITC-labeled Nanoemulsion FITC-KYF-Pt-NE

1. Synthesis of the KYF tripeptide and the fluorescently labeled tripeptide FITC-KYF
    1. Synthesize the KYF using standard solid-state peptide chemistry. Use the following standard coupling conditions to attach each amino acid: Wang resin (2.19 mmol), Fmoc protected amino acid (4.38 mmol), 2-(1H-Benzotriazole-1-yl)-1,1,3,3-tetramethylaminium tetrafluoroborate (TBTU) (4.38 mmol) and diisopropylethylamine (DIPEA) (8.76 mmol). Dissolve the amino acids with TBTU in dimethylformamide (DMF) and DIPEA.
    2. Soak 5.7 g of Fmoc-L-Phe 4-alkoxybenzyl alcohol resin (0.382 meq/g) in 25 mL of DMF for 1 h prior to use.
    3. Deprotect the amine group of L-phenylalanine amino acid with 15 mL of 20% piperidine/DMF solution for 5 min, discard the solvent and repeat the wash with 20 min cycle.
    4. Wash the resin for 1 min with the following solvents: DMF, isopropyl alcohol (IPA), DMF, IPA, DMF, IPA, DMF, DMF. Discard the solvent after each wash.
    5. Perform the Kaiser test to determine the presence of free NH_2 group on the resin (see substeps) and if positive (the resin seed is purple), add the Fmoc-L-tyrosine amino acid and perform the coupling overnight.
        1. Prepare Kaiser test solutions in separate bottles.
        2. Dissolve 5 g of ninhydrin in 100 mL of ethanol.
        3. Dissolve 80 g of phenol in 20 mL of ethanol.
        4. Mix 2 mL of 0.001 M aqueous solution of potassium cyanide with 98 mL of pyridine.
        5. Add 2-3 drops of each Kaiser test solutions to sample and heat in boiling water for 5 min.
    6. Upon successful coupling of second amino acid, perform the Kaiser test and if negative proceed with deprotection protocol (steps 2.1.3 to 2.1.5). Repeat the process with the Fmoc-phenylalanine amino acid.
        1. Upon coupling of all amino acids, wash the resin for 1 min with 5 mL of DMF, IPA, DMF, methanol, dichloromethane and diethyl ether, after each wash discard the solvent. Save the resin for further processing.
        2. Use half of the resin for the next steps (2.1.7-2.1.9) to modify the peptide with FITC. To obtain unmodified KYF tripeptide, follow the procedure starting at 2.1.10.
    7. Modify the N-terminal amino acid of the KYF to KYF-N_3 with 6-azidohexanoic acid. To this end, mix 1 g (0.382 mmol) of KYF Wang resin and 120.1 mg (0.764 mmol) of 6-azidohexanoic acid with 245.2 mg (0.764 mmol) of TBTU and 197.1 mg (1.528 mmol) of DIPEA in 30 mL of DMF. Stir the reaction overnight at room temperature.
    8. Obtain the KYF-FITC from the synthesis of the KYF-N_3 with propargyl fluorescein via a click reaction. To this end, mix 253 mg (0.097 mmol) of the KYF-N_3 Wang resin with 3.78 mg (0.019 mmol) of CuI solid, 71.9 mg (0.193 mmol) of propargyl fluorescein, and 2.24 mg (0.017 mmol) of DIPEA. The reaction should change color from green to brown.
    9. After 24 h, wash the resin for 1 min alternately with 5 mL of DMF and IPA five times, methanol and water thrice, DMF and water thrice, and with dichloromethane and diethyl ether thrice. Discard the solvent after each wash.
    10. Cleave the KYF-FITC or KYF peptide from the resin with a solution of trifluoroacetic acid (TFA)/triisopropylsilane (TIPS)/H_2O at the ratio of 95/2.5/2.5 over 3 hours.
    11. Precipitate the crude peptide in a cold diethyl ether, wash thrice with cold ether, and then dry under the vacuum.

2. Synthesis of FITC-KYF-stabilized nanoemulsion with Pt(II) (FITC-KYF-Pt-NE) and KYF-Pt-NE

1. Dissolve 10 mg (0.0126 mmol) of oleic acids–Pt(II) conjugate in 1.5 mL of isopropanol and place in a 5 mL syringe.
2. Place the syringe with oleic acids–Pt(II) conjugate in a syringe pump and set the flow to 0.1 mL/min.
3. In order to synthesize the FITC-KYF-Pt-NE, dissolve 1 mg (0.00105 mmol) of FITC-KYF and 1 mg (0.00219 mmol) of KYF (1:2 molar ratio of FITC-KYF:KYF) in 20 mL of water and adjust the temperature of the solution to 37 °C. Cover the walls of the container with aluminum foil to avoid photobleaching of the FITC fluorophore. To synthesize the KYF-Pt-NE, dissolve 2 mg (0.0044 mmol) of KYF tripeptide in 20 mL of water and adjust the temperature of the solution to 37 °C.
4. Add the oleic acids–Pt(II) conjugate dropwise to the solution of FITC-KYF/KYF or KYF tripeptide. Perform this step under the hood.
5. Stir the solution overnight at room temperature to evaporate organic solvents and to allow the self-assembly of FITC-KYF-Pt-NE or KYF-Pt-NE.
6. Concentrate the FITC-KYF-Pt-NE or KYF-Pt-NE in a centrifugal concentrator (10k MWCO), and wash thrice with 4 mL of the nanopure water.
7. Store the aqueous solutions of KYF-Pt-NE and FITC-KYF-Pt-NE at 4 °C.
8. Analyze for platinum content using atomic absorption spectroscopy (AAS), following the manufacturer's guide[48].
    1. Prepare platinum standards in 10% HCl solution for the calibration curve (effective range for AAS is between 100 to 1200 ppb (parts per billion)).
    2. Dissolve 50 µL of KYF-Pt-NE solution from step 2.2 in 100 µL of aqua regia (a mixture 3:1 of concentrated hydrochloric acid and nitric acid) and leave at room temperature overnight. Add 850 µL of water to reach a final sample volume of 1 mL. Analyze the sample using AAS. The final acid concentration should be 10% in all analyzed samples.
    3. Record the reading of Pt concentration in ppb, and compute the final platinum content in the sample (account for sample dilution and initial volume of nanoemulsion).

3. Confocal Imaging of the Cellular Uptake of FITC-KYF-Pt-NE

1. Seed 6 ovarian cancer cell lines (A2780, CP70, SKOV3, OV90, TOV21G, and ES2), into 4 well-chamber confocal dishes at the density of 4.7 x 10^4 cells per chamber, and pre-culture overnight at 37 °C.
2. After 24 h, wash the cells thrice with phosphate buffer saline (PBS) and incubate with FITC-KYF-Pt-NE in cell culture medium (see step 6.1 for cell line specific details) for 15 min at 37 °C.
3. After incubation, remove the media and wash the cells three times with PBS.
4. Fix the cells with cold methanol for 5 min at -20 °C and wash three times with 1 mL of PBS.
5. Permeabilize the cells with 1 mL of 0.1% Triton-X for 10 min at room temperature and wash three times with 1 mL of PBS.
6. Incubate the cells for 90 min with LAMP1 antibody conjugated with Alexa Fluor 647 (1 mL) at 1:50 dilution in PBS at room temperature. Next, wash the cells 3 times with PBS.
7. Dilute DAPI stock solution (1 mg/mL) to 1 mg/mL in PBS. Then, add 1 mL of the diluted solution to each chamber and incubate for 15 min at room temperature. Wash the cells 3 times with PBS.
8. Mount coverslips on a slide using mounting medium.
9. Image the cells using live cell confocal microscope at excitation wavelength of 405 nm, 488 nm and 633 nm. Set the detection parameters as follow: laser power from 0.2% and no more than 1%, Pinole 1 Airy unit, Gain master 650-750, Digital offset 0.
10. Open image in imaging software. Under displayed image, select **Graphics** and select **Insert Scale Bar**, to insert the scale bar to the image.

4. Drug Release Studies

1. Carry out the drug release studies in PBS. Adjust the pH values of three PBS buffers to 7.4, 6.8 and 5.0 respectively.
2. Dilute 5 µL of KYF-Pt-NE in 180 µL of appropriate pH PBS buffer, transfer to 3.5 kDa MWCO mini dialysis cup and incubate at 37 °C in PBS.
3. Remove buffer from each three mini dialysis tubes at 2, 4, 6, 24, 48, and 140 h, and measure the platinum concentrations by AAS. Prepare all samples according to step 2.2.8 but adjust the final volume of the sample to 500 µL.

5. Cell Culture Methods

1. Culture cell lines A2780, CP70, SKOV-3, OV-90, TOV-21G, ES-2 in cell culture medium (DMEM) supplemented with 10% (A2780, CP70, SKOV-3, ES-2) or with 15% (TOV-21G, OV-90) fetal bovine serum (FBS), with L-Glutamine and penicillin/streptomycin. Grow all cells in a 5% CO_2, water saturated atmosphere at 37 °C.
2. Seed 3 x 10^5 cells in each 96-well plate and pre-culture overnight for in vitro incubation experiments. Prepare the KYF-Pt-NE, cisplatin, and carboplatin solutions in water. Adjust the concentration of Pt(II) in KYF-Pt-NE to match the concentration of carboplatin and cisplatin for each cell line. Incubate for 72 hours at 37 °C.
3. After incubation, evaluate the cellular viability using a colorimetric assay (the MTT Cell Proliferation assay). Briefly, remove medium and add 110 µL of 10% MTT in medium to each well and incubate for 2 h at 37 °C. Then add 100 µL detergent to each well and incubate for 5 h at 37 °C.
4. Check the absorbance at 570 nm by using plate reader. Analyze results using statistical analysis with Z-test and P-test.

Representative Results

Representative TEM image of KYF-Pt-NE prepared using this protocol is shown in **Figure 2A**. The KYF-Pt-NEs are spherical in morphology, well dispersed, and uniform in size. The core diameter of the KYF-Pt-NEs, measured directly from three TEM images with a minimum of 200 measurements done, is 107 ± 27 nm. The hydrodynamic diameter of KYF-Pt-NE, analyzed using dynamic light spectroscopy (DLS), was found to be 240 nm with a polydispersity index of 0.156. The Zeta potential of KYF-Pt-NE in water was determined for three independent syntheses with the average value of -60.1 mV. The high magnitude of the potential indicates good colloidal stability of the formulation, and the negative surface charge is attributed to ionized COO^- surface groups of oleic acids. The isoelectric point of KYF is 8.59, and therefore it is positively charged at neutral pH.

The ability of the nanoemulsions to cross the cellular membrane was examined using the fluorescently labeled FITC-KYF-Pt-NE and ovarian cancer cell lines. The results are presented in **Figure 2B**. It can be clearly seen that the FITC-KYF-Pt-NEs (green) are distributed within the cytosol but were not yet associated with lysosomes (red). This result demonstrates that KYF-Pt-NEs enter cells and can serve as intracellular drug delivery vehicle.

The stability of KYF-Pt-NEs and FITC-KYF-Pt-NEs was assessed with DLS. The diameter of the nanoemulsions in water was measured over several months and the results are presented in **Figure 3**. The hydrodynamic diameter of both formulations slowly increased during 4 months in storage, to 320 nm (KYF-Pt-NE) and 240 nm (FITC-KYF-Pt-NE), but the nanoscale dimensions were preserved. This result suggests that the KYF tripeptide effectively stabilizes nanoemulsions over long periods of time.

The Pt(II) encapsulation efficiency and release from the nanoemulsion were measured with AAS. The Pt(II) concentration in KYF-Pt-NE was established to be 10 wt.%. The Pt(II) release from KYF-Pt-NE at pH 7.4 (physiological), 6.8 (tumor's interstitium)[49], and 5.0 (endosomal)[50] is presented in **Figure 4A**. The Pt(II) release is the slowest at pH 7.4 with only 20.8% of Pt(II) released after 4 h, while at pH 6.8 and 5.0 the release was 32.8% of and 47.5%, respectively. The same trend continued after 24 h and after 6 days. This result indicates that Pt(II) release from KYF-Pt-NE is pH dependent, and it can be delayed in the systemic circulation, and accelerated once the nanoemulsions translocate into tumor.

The biological activity of the KYF-Pt-NE was established in vitro using the same ovarian cancer cell lines as in the imaging studies. The cells were incubated with KYF-Pt-NE for 72 h, at KYF-Pt-NE concentrations corresponding to IC_{50} for each cell line. The viability was assessed using the MTT assay and the results were compared to cells only, KYF-NE, oleic acids-Pt(II) conjugate, carboplatin, and cisplatin. The results of biological activity of KYF-Pt-NE are shown in **Figure 4B**. The KYF-Pt-NE reduced the viability of isogenic cell lines A2780 (Pt sensitive) and CP70 (Pt resistant) by 44.3% and 46.2% respectively. Carboplatin, the clinically relevant analogue, decreased the viability by 18.5% (A2780) and 9.6% (CP70) only. The same trend of greater KYF-Pt-NE effect on cell death was observed across other cell lines as well. The viability of Pt(II) sensitive TOV-21G cells was reduced by 55.9% after incubation with KYF-Pt-NE, while carboplatin resulted in lowering the viability by just 16.5%. In OV-90 cells with intermediate Pt(II) resistance, the viability was lowered by 55.3% (KYF-Pt-NE) and 23.9% (carboplatin). The two resistant cancer cell lines, ES-2 and SKOV-3, showed reduction in viability by 45.9% and 54.3%, respectively, for KYF-Pt-NE, and 10.3% (ES-2) and 16.8% (SKOV-3) for carboplatin.

The biological activity of KYF-Pt-NE versus cisplatin was also compared. Cisplatin is the Pt(II)-based agent of first generation that is no longer favored in the clinic due to its toxicity profile[51]. In two cell lines, SKOV-3 and TOV-21G, the viability reduction was greater by 15% and 40%, respectively, for KYF-Pt-NE than for cisplatin. In the remaining cell lines, the activity of KYF-Pt-NE was comparable to cisplatin (A2780, CP70, OV-90), or slightly lower (ES-2). The oleic acids-Pt(II) conjugate was also found to be biologically active. However, KYF-Pt-NE showed higher reduction in viability than the conjugate in majority of the cell lines tested, indicating the significance of nanoformulation in Pt(II) activity.

The biological applications of nanoparticulate systems require stability in biologically relevant media, thus the stability of KYF-Pt-NE was evaluated in 20% fetal bovine serum (FBS) and the results are presented in **Figure 4C**. We detected no evidence of KYF-Pt-NE opsonization in serum after one day of incubation.

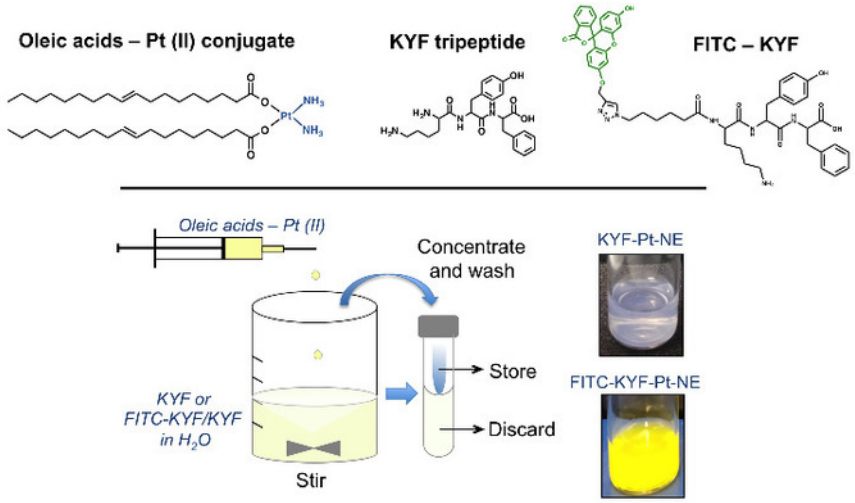

Figure 1. The components of the nanoemulsions (top) and schematic of the nanoemulsion preparation (bottom). Please click here to view a larger version of this figure.

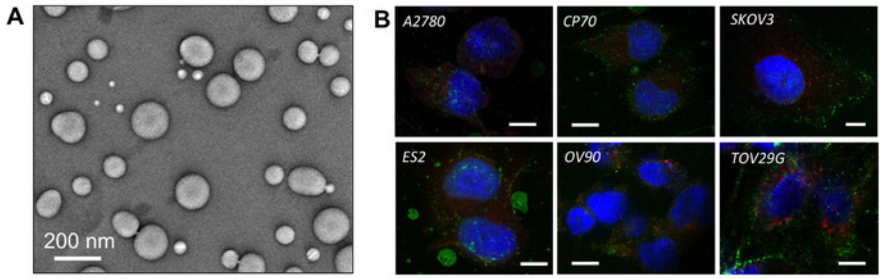

Figure 2. TEM image of KYF-Pt-NE (A) and confocal microscope images of FITC-KYF-Pt-NE (green) uptake by ovarian cancer cells (nuclei are blue and lysosomes are red) (**B**). Scale bars are 10 µm. This Figure has been adapted with permission from *Bioconjugate Chemistry* 2018, 29, 2514-2519.[46] Copyright 2018 American Chemical Society. Please click here to view a larger version of this figure.

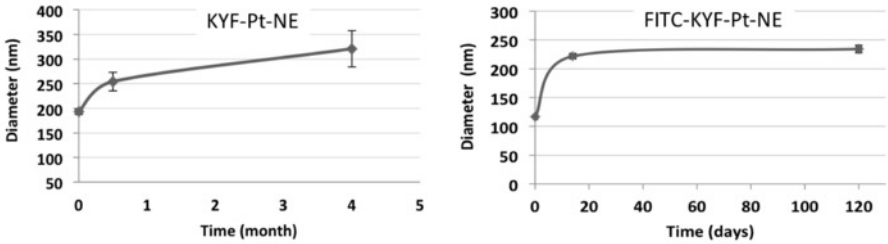

Figure 3. Stability of KYF-Pt-NE and FITC-KYF-Pt-NE in water. Each point represents the mean and standard deviation of N=3 and $p < 0.005$. This Figure has been adapted with permission from *Bioconjugate Chemistry* 2018, 29, 2514-2519.[46] Copyright 2018 American Chemical Society. Please click here to view a larger version of this figure.

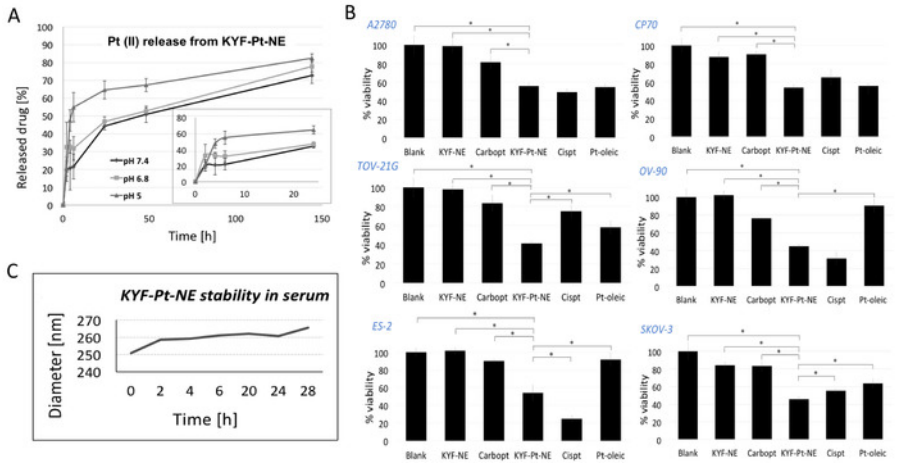

Figure 4. KYF-Pt-NE stability and biological activity. (**A**) Pt(II) release from KYF-Pt-NE in PBS buffer at different pHs (PBS, 37 °C). Cellular viability of different ovarian cancer cell lines after 72 h incubation with KYF-Pt-NE (**B**). Each column represents the mean and standard deviation of N=3 and p <0.005. The concentrations are constant in each cell line and are as follows: 4.92 mM (A2780), 8.80 mM (CP70), 2.46 mM (TOV-21G), 9.84 mM (SKOV3), 7.38 mM (ES-2), 19.7 mM (OV-90). The concentration of KYF-Pt-NE and oleic acids–Pt(II) conjugate was adjusted with respect to Pt(II) content measured by AAS. Abbreviations: "Carbpt" – carboplatin; "KYF-NE" – KYF tripeptide-coated nanoemulsion; "KYF-Pt-NE" – KYF tripeptide-coated nanoemulsion containing Pt(II); Cispt – cisplatin; Pt-oleic – oleic acids–Pt(II) conjugate. (**C**) KYF-Pt-NE stability in serum. This Figure has been adapted with permission from *Bioconjugate Chemistry* 2018, 29, 2514-2519.[46] Copyright 2018 American Chemical Society. Please click here to view a larger version of this figure.

Discussion

Critical steps in the nanoemulsion synthesis include adjusting the molar ratio of the substrates, maintaining temperature and flow rate control during oleic acids–Pt(II) addition, providing sufficient time for self-assembly, and purifying the product using a centrifugal concentrator column. These parameters influence the size and morphology of the KYF-Pt-NE; thus, it is particularly important to maintain the proper molar ratio and adjust the synthetic conditions correctly.

The ratio of the substrates during the nanoemulsion synthesis (step 3) is crucial for the self-assembly process and determines the final size of the product. The KYF to oleic acid-Pt(II) molar ratio is 1:3, and the optimal concentration of the KYF tripepide in water is 0.2 mM. In addition, the organic solvent used to dissolve the oleic acid-Pt(II) conjugate in step 3.1 has to be miscible with water, compatible with the filtration system, and evaporative easily at room temperature.

One of the critical steps is the dropwise addition of the oleic acid-Pt(II) conjugate to the KYF solution (step 3.4). The flow should not be slower than 0.1 mL/min and not faster than 0.2 mL/min, because a sub-optimal speed can induce the precipitation of the nanoemulsion. Also, the oleic acids–Pt(II) conjugate should be added to the KYF solution at 37 °C while stirring the mixture on a stir plate at 600 rpm. Once all of the oleic acid-Pt(II) has been added, the solution should be kept at room temperature and the stirring speed reduced to 150 rpm. Step 3.5 should be carried out at room temperature. The optimal time for the self-assembly of the KYF-Pt-NE (step 3.5) is 24 hours.

There is a risk that the product may precipitate while the nanoemulsion is being pre-concentrated. Therefore, it is recommended that the nanoemulsion be diluted with additional water before being centrifuged in a centrifugal concentrator and spun no faster than 2,465 x *g*. The diluted nanoemulsions should be added to the centrifugal concentrator at aliquots between spins, and the nanoemulsion should be mixed in the filter before the next portion is added.

The ability to form nanoemulsions with fatty acids derivatives other than oleic acid has not been tested and is yet to be determined. Future applications may include the use of different peptides to facilitate the co-assembly with oleic acid. Also, oleic acid conjugates with non-platinum-based drugs may be used as potential cores of nanoemulsions.

Disclosures

Authors do not have a conflict of interest to disclose.

Acknowledgements

We gratefully acknowledge financial support from the National Cancer Institute, grant SC2CA206194. No competing financial interests are declared.

References

1. Agrahari, V., Agrahari, V., Mitra, A. K. Nanocarrier fabrication and macromolecule drug delivery: challenges and opportunities. *Therapeutic Delivery.* **7** (4), 257-278 (2016).
2. Anselmo, A. C., Mitragotri, S. Nanoparticles in the clinic. *Bioengineering & Translational Medicine.* **1** (1), 10-29 (2016).
3. Peer, D., Karp, J. M., Hong, S., Farokhzad, O. C., Margalit, R., Langer, R. Nanocarriers as an emerging platform for cancer therapy. *Nature Nanotechnology.* **2** (12), 751-760 (2007).
4. Roy Chowdhury, M., Schumann, C., Bhakta-Guha, D., Guha, G. Cancer nanotheranostics: Strategies, promises and impediments. *Biomedicine & Pharmacotherapy.* **84**, 291-304 (2016).
5. Jeevanandam, J., Chan, Y. S., Danquah, M. K. Nano-formulations of drugs: Recent developments, impact and challenges. *Biochimie.* **128-129**, 99-112 (2016).
6. Meerum Terwogt, J. M., Groenewegen, G., Pluim, D., Maliepaard, M., Tibben, M. M., Huisman, A., ten Bokkel Huinink, W. W., Schot, M., Welbank, H., Voest, E. E., Beijnen, J. H., Schellens, J. M. Phase I and pharmacokinetic study of SPI-77, a liposomal encapsulated dosage form of cisplatin. *Cancer Chemotherapy and Pharmacology.* **49** (3), 201-210 (2002).
7. Fan, Z., Sun, L., Huang, Y., Wang, Y., Zhang, M. Bioinspired fluorescent dipeptide nanoparticles for targeted cancer cell imaging and real-time monitoring of drug release. *Nature Nanotechnology.* **11** (4), 388-394 (2016).
8. Jeong, Y. et al. Enzymatically degradable temperature-sensitive polypeptide as a new in-situ gelling biomaterial. *Journal of Controlled Release.* **137** (1), 25-30 (2009).
9. Uesaka, A. et al. Morphology control between twisted ribbon, helical ribbon, and nanotube self-assemblies with his-containing helical peptides in response to pH change. *Langmuir.* **30** (4), 1022-1028 (2014).
10. Hwang, W., Marini, D. M., Kamm, R. D., Zhang, S. Supramolecular structure of helical ribbons self-assembled from a B-sheet peptide. *Journal of Chemical Physics.* **118** (1), 389-397 (2003).
11. Svobodova, J. et al. Poly(amino acid)-based fibrous scaffolds modified with surface-pendant peptides for cartilage tissue engineering. *Journal of Tissue Engineering and Regenerative Medicine.* **11** (3), 831-842 (2017).
12. Kumar, V. A. et al. Highly angiogenic peptide nanofibers. *ACS Nano.* **9** (1), 860-868 (2015).
13. Romera, D., Couleaud, P., Mejias, S. H., Aires, A., Cortajarena, A. L. Biomolecular templating of functional hybrid nanostructures using repeat protein scaffolds. *Biochemical Society Transactions.* **43** (5), 825-831 (2015).
14. Medina, S. H., Schneider, J. P. Cancer cell surface induced peptide folding allows intracellular translocation of drug. *Journal of Controlled Release.* **209**, 317-326 (2015).
15. Recio, C., Maione, F., Iqbal, A. J., Mascolo, N., De Feo, V. The Potential Therapeutic Application of Peptides and Peptidomimetics in Cardiovascular Disease. *Frontiers in Pharmacology.* **7**, 526 (2016).
16. McCarthy, K. A. et al. Phage Display of Dynamic Covalent Binding Motifs Enables Facile Development of Targeted Antibiotics. *Journal of the American Chemical Society.* **140** (19), 6137-6145 (2018).
17. Lazar, V. et al. Antibiotic-resistant bacteria show widespread collateral sensitivity to antimicrobial peptides. *Nature Microbiology.* **3** (6), 718-731 (2018).
18. Czeczor, J. K., McGee, S. L. Emerging roles for the amyloid precursor protein and derived peptides in the regulation of cellular and systemic metabolism. *Journal of Neuroendocrinology.* **29** (5) (2017).
19. Branco, M. C., Sigano, D. M., Schneider, J. P. Materials from peptide assembly: towards the treatment of cancer and transmittable disease. *Current Opinion in Chemical Biology.* **15** (3), 427-434 (2011).
20. Cheetham, A. G. et al. Targeting Tumors with Small Molecule Peptides. *Current Cancer Drug Targets.* **16** (6), 489-508 (2016).
21. Ndinguri, M. W., Solipuram, R., Gambrell, R. P., Aggarwal, S., Hammer, R. P. Peptide targeting of platinum anti-cancer drugs. *Bioconjugate Chemistry.* **20** (10), 1869-1878 (2009).
22. Eskandari, S., Guerin, T., Toth, I., Stephenson, R. J. Recent advances in self-assembled peptides: Implications for targeted drug delivery and vaccine engineering. *Advanced Drug Delivery Reviews.* **110-111**,. 169-187 (2017).
23. Zhou, J., Du, X., Yamagata, N., Xu, B. Enzyme-Instructed Self-Assembly of Small D-Peptides as a Multiple-Step Process for Selectively Killing Cancer Cells. *Journal of the American Chemical Society.* **138** (11), 3813-3823 (2016).
24. Sun, J. E. et al. Sustained release of active chemotherapeutics from injectable-solid beta-hairpin peptide hydrogel. *Biomaterials Science.* **4** (5), 839-848 (2016).
25. Lock, L. L., Reyes, C. D., Zhang, P., Cui, H. Tuning Cellular Uptake of Molecular Probes by Rational Design of Their Assembly into Supramolecular Nanoprobes. *Journal of the American Chemical Society.* **138** (10), 3533-3540 (2016).
26. Kalafatovic, D., Nobis, M., Son, J., Anderson, K. I., Ulijn, R. V. MMP-9 triggered self-assembly of doxorubicin nanofiber depots halts tumor growth. *Biomaterials.* **98**, 192-202 (2016).
27. Frederix, P. W. et al. Exploring the sequence space for (tri-)peptide self-assembly to design and discover new hydrogels. *Nature Chemistry.* **7** (1), 30-37 (2015).
28. Horsley, J. R. et al. Photoswitchable peptide-based 'on-off' biosensor for electrochemical detection and control of protein-protein interactions. *Biosensors and Bioelectronics.* **118**, 188-194 (2018).
29. Hoyos-Nogues, M., Gil, F. J., Mas-Moruno, C., Antimicrobial Peptides: Powerful Biorecognition Elements to Detect Bacteria in Biosensing Technologies. *Molecules.* **23** (7), 1683 (2018).
30. Xiao, X. et al. Advancing Peptide-Based Biorecognition Elements for Biosensors Using in-Silico Evolution. *ACS Sensors.* **3** (5), 1024-1031 (2018).
31. Puiu, M., Bala, C. Peptide-based biosensors: From self-assembled interfaces to molecular probes in electrochemical assays. *Bioelectrochemistry.* **120**, 66-75 (2018).
32. Wang, J. et al. Developing a capillary electrophoresis based method for dynamically monitoring enzyme cleavage activity using quantum dots-peptide assembly. *Electrophoresis.* **38** (19), 2530-2535 (2017).
33. Etayash, H., Thundat, T., Kaur, K. Bacterial Detection Using Peptide-Based Platform and Impedance Spectroscopy. *Methods in Molecular Biology.* **1572**, 113-124 (2017).
34. Handelman, A., Apter, B., Shostak, T., Rosenman, G. Peptide Optical waveguides. *Journal of Peptide Science.* **23** (2), 95-103 (2017).

35. Chen, C., Liu, K., Li, J., Yan, X. Functional architectures based on self-assembly of bio-inspired dipeptides: Structure modulation and its photoelectronic applications. *Advances in Colloid and Interface Science.* **225**, 177-193 (2015).
36. Reddy, S. M., Shanmugam, G. Role of Intramolecular Aromatic pi-pi Interactions in the Self-Assembly of Di-l-Phenylalanine Dipeptide Driven by Intermolecular Interactions: Effect of Alanine Substitution. *Chemphyschem.* **17** (18), 2897-2907 (2016).
37. Marchesan, S. et al. Unzipping the role of chirality in nanoscale self-assembly of tripeptide hydrogels. *Nanoscale.* **4** (21), 6752-6760 (2012).
38. Scott, G. G., McKnight, P. J., Tuttle, T., Ulijn, R. V. Tripeptide Emulsifiers. *Advanced Materials.* **28** (7), 1381-1386 (2016).
39. Galanski, M., Jakupec, M. A., Keppler, B. K. Update of the preclinical situation of anticancer platinum complexes: novel design strategies and innovative analytical approaches. *Current Medicinal Chemistry.* **12** (18), 2075-94 (2005).
40. Wheate, N. J., Walker, S., Craig, G. E., Oun, R. The status of platinum anticancer drugs in the clinic and in clinical trials. *Dalton Transactions.* **39** (35), 8113-8127 (2010).
41. Oberoi, H. S., Nukolova, N. V., Kabanov, A. V., Bronich, T. K. Nanocarriers for delivery of platinum anticancer drugs. *Advanced Drug Delivery Reviews.* **65** (13-14), 1667-1685 (2013).
42. Fichtinger-Schepman, A. M., van Oosterom, A. T., Lohman, P. H., Berends, F. cis-Diamminedichloroplatinum(II)-induced DNA adducts in peripheral leukocytes from seven cancer patients: quantitative immunochemical detection of the adduct induction and removal after a single dose of cis-diamminedichloroplatinum(II). *Cancer Research.* **47** (11), 3000-3004 (1987).
43. Englander, E. W. DNA damage response in peripheral nervous system: coping with cancer therapy-induced DNA lesions. *DNA Repair.* **12** (8), 685-690 (2013).
44. Galluzzi, L. et al. Molecular mechanisms of cisplatin resistance. *Oncogene.* **31** (15), 1869-1883 (2012).
45. Boeckman, H. J., Trego, K. S., Turchi, J. J. Cisplatin sensitizes cancer cells to ionizing radiation via inhibition of nonhomologous end joining. *Molecular Cancer Research.* **3** (5), 277-285 (2005).
46. Dragulska, S. A. et al. Tripeptide-Stabilized Oil-in-Water Nanoemulsion of an Oleic Acids-Platinum(II) Conjugate as an Anticancer Nanomedicine. *Bioconjugate Chemistry.* **29** (8), 2514-2519 (2018).
47. Martinez Rivas, C. J. et al. Nanoprecipitation process: From encapsulation to drug delivery. *International Journal of Pharmaceutics.* **532** (1), 66-81 (2017).
48. Agilent Technologies. *Analytical Methods for Graphite Tube Atomizers, User's Guide Manual, 8th edition.* (2012).
49. Park, S. Y. et al. A smart polysaccharide/drug conjugate for photodynamic therapy. *Angewandte Chemie.* **50** (7), 1644-1647 (2011).
50. Canton, I., Battaglia, G. Endocytosis at the nanoscale. *Chemical Society Reviews.* **41** (7), 2718-2739 (2012).
51. Lokich, J., Anderson, N. Carboplatin versus cisplatin in solid tumors: an analysis of the literature. *Annals of Oncology.* **9** (1), 13-21 (1998).

